J. Fluid Mech. (1994), *vol.* 269, *pp.* 301–321

An analytical theory of distributed axisymmetric barotropic vortices on the β-plane

By G. M. REZNIK[1] AND W. K. DEWAR[2]

[1] P. P. Shirshov Institute of Oceanology, Russian Academy of Sciences, Krasikova, 23, Moscow 117218, Russia

[2] Department of Oceanography, Geophysical Fluid Dynamics Institute and Supercomputer Computations Research Institute, Florida State University, Tallahassee, FL 32306, USA

(Received 30 June 1993 and in revised form 3 January 1994)

An analytical theory of barotropic β-plane vortices is presented in the form of an asymptotic series based on the inverse of vortex nonlinearity. In particular, a solution of the initial value problem is given, in which the vortex is idealized as a radially symmetric function of arbitrary structure. Motion of the vortex is initiated by its interaction with the so-called 'β-gyres' which, in turn, are generated by the vortex circulation. Comparisons of analytical and numerical predictions for vortex motion are presented and demonstrate the utility of the present theory for times comparable to the 'wave' timescale. The latter exceeds the temporal limit derived from formal considerations. The properties of the far-field planetary wave radiation are also computed.

This theory differs from previous calculations by considering more general initial vortex profiles and by obtaining a more complete solution for the perturbation fields. Vortex trajectory predictions accrue error systematically by integrating vortex propagation rates which are too strong. This appears to be connected to higher-order planetary wave radiation effects.

1. Introduction

There is by now a wide literature concerning the evolution of intense barotropic vortices on the β-plane, especially in connection with the theory of tropical cyclones. The physics of this evolution (for not very large times) is now clear: the β-plane effect creates a secondary dipole circulation (the so-called β-gyres) which interacts with the vortex and forces it to move along the dipole axis. This axis rotates owing to the vortex circulation. The sense of this rotation is determined by the sense of the vortex; i.e. counterclockwise (clockwise) for cyclonic (anticyclonic) vortices.

Thus, a cyclonic (anticyclonic) vortex moves northwestward (southwestward) along some curved trajectory. Such motion is accompanied by planetary wave radiation which, at first, rather weakly influences the vortex trajectory (i.e. for times of the order of $(\beta L)^{-1}$, where β is the meridional gradient of the Coriolis parameter and L is a characteristic vortex lengthscale). On times larger than $O(\beta L)^{-1}$, the influence of planetary wave radiation is not well understood, but probably cannot be neglected. In part, this is because of its influence upon the net angular momentum of the vortex. This somewhat simplified scheme has been confirmed in the laboratory (cf. Firing & Beardsley 1976) and in several numerical experiments (cf. McWilliams & Flierl 1979; Fiorino & Elsberry 1989; Shapiro & Ooyama 1990; Ross & Kurihara 1992).

Some related analytical work also has been done. Adem (1956) investigated the

initial generation of β-gyres, for times much smaller than the vortex turnover time. Sutyrin (1988, 1989) derived equations governing the joint evolution of the axisymmetrical part of an intense initially circular vortex and its β-gyres. These equations are valid for times larger than the vortex turnover time and can be used to calculate the vortex trajectory for times of $O(\beta L)^{-1}$.

Some progress was also achieved in the theory of singular monopolar vortices. Since the inner structure of such a vortex is fixed and very simple, the equations describing its evolution can be solved analytically in some cases. Bogomolov (1977, 1979, 1985) investigated the initial motion of a non-divergent point vortex on the rotating sphere and Reznik (1990, 1992) suggested a theory of singular vortices on the β-plane. One of the results of this theory is the analytical description of the evolution of an intense divergent singular vortex valid on times much larger than the turnover time. Reznik & Kravtsov (1994) developed the analogous theory for the non-divergent singular vortices on the β-plane and obtained simple analytical expressions for vortex trajectory and the time-dependent β-gyres.

The analytical description of a distributed vortex is more complicated than that of a singular vortex, because of the inner structure of the former. One difficulty is that the vortex trajectory cannot be uniquely defined; rather, it must be chosen and in principle depends on this choice. For example, we may choose to track the point of maximum pressure, the vorticity extremum or some fluid particle within the vortex core. The tracks of these points may differ from each other. Also, the equation for the β-gyres, although linear, is generally too complicated to solve analytically. Some special cases have proven to be tractable; Sutyrin & Flierl (1994), for example, successfully considered a vortex with piecewise-uniform potential vorticity.

In spite of these difficulties an analytical theory of barotropic β-plane vortices, based on an approximate equation, has been proposed by Smith & Ulrich (1990) and Smith & Weber (1993). In order to proceed, however, they simplified the dynamics of the β-gyres, employed some *ad hoc* assumptions and used an iterative procedure (see below). Nonetheless, comparisons with numerical results have demonstrated that their theory accurately predicts vortex trajectories and the β-gyres for times $t \lesssim (\beta L)^{-1}$.

We present here an analytical theory of intense non-divergent barotropic vortices on the β-plane. This theory differs from the those above in that it considers distributed vortices, as opposed to singular vortices and is not restricted to the uniform potential vorticity distributions of Flierl and Sutyrin. Finally, we have been able to avoid the *ad hoc* approximations made by Smith and collaborators. Section 2 contains a statement of the problem. The solution for the β-gyres is derived in §3. In §4, various definitions of the vortex trajectory and velocity are discussed. Asymptotic regimes valid at large distances from the vortex centre and at large times compared to the vortex turnover time are investigated in §5. Section 6 contains a comparison of the theory with numerical experiments, and the circulation in the far-field caused by planetary wave radiation from the vortex is described in §7. A discussion of the results concludes the paper. Some useful formulae and an analytical demonstration of the linear f-plane stability of an arbitrary barotropic vortex to mode-1 perturbations are given in Appendices A and B.

2. Governing equations

We consider the initial value problem governed by the well-known barotropic potential vorticity equation (cf. Pedlosky 1986)

$$\frac{\partial \nabla^2 \psi}{\partial t} + \beta \frac{\partial \psi}{\partial x} + J(\psi, \nabla^2 \psi) = 0, \tag{2.1}$$

where ψ denotes streamfunction; x, y eastward and northward coordinates respectively; t time; ∇^2 the Laplacian operator and J the usual Jacobian operator. We take as an initial condition for (2.1) an axisymmetrical localized vortex, i.e.

$$\psi(t=0) = \psi_0(r), \tag{2.2}$$

where $r = (x^2+y^2)^{\frac{1}{2}}$.

If $\beta = 0$, the initial state (2.2) is a stationary solution of (2.1). Under the influence of β, the vortex (2.2) moves along some trajectory $\boldsymbol{r} = (\bar{X}(t), \bar{Y}(t))$, with a velocity

$$\boldsymbol{U} = (U(t), V(t)) = \left(\frac{\mathrm{d}}{\mathrm{d}t}\bar{X}, \frac{\mathrm{d}}{\mathrm{d}t}\bar{Y}\right)$$

and also excites planetary waves. In the moving coordinate system defined by $x' = x - X(t)$, $y' = y - Y(t)$, (2.1) takes the form

$$\frac{\partial \nabla^2 \psi}{\partial t} - U\frac{\partial \nabla^2 \psi}{\partial x} - V\frac{\partial \nabla^2 \psi}{\partial y} + \beta \frac{\partial \psi}{\partial x} + J(\psi, \nabla^2 \psi) = 0, \tag{2.3}$$

where primes are omitted. Since the vortex motion is caused by β, the second, third and fourth terms in (2.3) must be of the same order, whence it follows that the velocities U, V scale as

$$U_* = \beta L^2, \tag{2.4}$$

where L is a vortex lengthscale.

Denoting the scale of the vortex swirl velocity by U_v, the streamfunction is expected to scale as $\psi_* = U_v L$ and the eddy turnover time as $T_* = L/U_v$. Thus the non-dimensional form of (2.1) is

$$\frac{\partial \nabla^2 \psi}{\partial t} + J(\psi, \nabla^2 \psi) + \alpha\left(-U\frac{\partial \nabla^2 \psi}{\partial x} - V\frac{\partial \nabla^2 \psi}{\partial y} + \frac{\partial \psi}{\partial x}\right) = 0, \tag{2.5}$$

where $\alpha = U_*/U_v = \beta L^2/U_v$.

3. Intense vortex structure

Consider now the case of an intense vortex, defined by

$$\alpha = U_*/U_v \ll 1. \tag{3.1}$$

The solution to the problem (2.2), (2.5) and (3.1) is sought in the form of an asymptotic expansion in α:

$$\psi = \psi_0(r) + \alpha\psi_1(r,t) + \alpha^2\psi_2(r,t) + \ldots, \tag{3.2}$$

$$\boldsymbol{U} = \boldsymbol{U}_0(t) + \alpha \boldsymbol{U}_1(t) + \ldots \tag{3.3}$$

(cf. Peng & Williams 1990). Substitution of (3.2) and (3.3) into (2.2) and (2.5) gives

$$\frac{\partial \nabla^2 \psi_1}{\partial t} + J(\psi_0, \nabla^2 \psi_1) + J(\psi_1, \nabla^2 \psi_0) - U_0\frac{\partial \nabla^2 \psi_0}{\partial x} - V_0\frac{\partial \nabla^2 \psi_0}{\partial y} + \frac{\partial \psi_0}{\partial x} = 0; \tag{3.4a}$$

$$\frac{\partial \nabla^2 \psi_2}{\partial t} + J(\psi_0, \nabla^2 \psi_2) + J(\psi_2, \nabla^2 \psi_0) + J(\psi_1, \nabla^2 \psi_1)$$

$$- U_0\frac{\partial \nabla^2 \psi_1}{\partial x} - V_0\frac{\partial \nabla^2 \psi_1}{\partial y} + \frac{\partial \psi_1}{\partial x} - U_1\frac{\partial \nabla^2 \psi_0}{\partial x} - V_1\frac{\partial \nabla^2 \psi_0}{\partial y} = 0; \tag{3.4b}$$

$$\psi_1(t=0) = 0, \quad \psi_2(t=0) = 0. \tag{3.4c, d}$$

Equations (3.4a, c) are non-constant, but nonetheless linear, equations; therefore, their solution can be represented in the form

$$\psi_1 = \hat{\psi}_1 + \hat{\psi}_2, \tag{3.5}$$

where $\hat{\psi}_1$ and $\hat{\psi}_2$ satisfy

$$\frac{\partial \nabla^2 \hat{\psi}_1}{\partial t} + J(\psi_0, \nabla^2 \hat{\psi}_1) + J(\hat{\psi}_1, \nabla^2 \psi_0) = -\frac{\partial \psi_0}{\partial x}, \tag{3.6a}$$

$$\frac{\partial \nabla^2 \hat{\psi}_2}{\partial t} + J(\psi_0, \nabla^2 \hat{\psi}_2) + J(\hat{\psi}_2, \nabla^2 \psi_0) = U_0 \frac{\partial \nabla^2 2\psi_0}{\partial x} + V_0 \frac{\partial \nabla^2 \psi_0}{\partial y}, \tag{3.6b}$$

with initial conditions

$$\hat{\psi}_i(t = 0) = 0, \quad i = 1, 2. \tag{3.6c}$$

The solution to (3.6b, c) is readily found and has the form

$$\hat{\psi}_2 = \bar{X}_0 \frac{\partial \psi_0}{\partial x} + \bar{Y}_0 \frac{\partial \psi_0}{\partial y}, \tag{3.7a}$$

where

$$(\bar{X}_0, \bar{Y}_0) = \int_0^t (U_0, V_0)\, \mathrm{d}t. \tag{3.7b}$$

To solve (3.6a) we employ polar coordinates (r, θ), yielding

$$\frac{\partial \nabla^2 \hat{\psi}_1}{\partial t} + J(\psi_0, \nabla^2 \hat{\psi}_1) + J(\hat{\psi}_1, \nabla^2 \psi_0) = -\psi_0' \cos\theta, \tag{3.8}$$

where the prime denotes differentiation with respect to r. The general solution to (3.8) involves a homogeneous and an inhomogeneous part. The former can be neglected in view of the initial condition. It is a simple matter to show that the inhomogeneous part involves only the sum of the two dipole components,

$$\hat{\psi}_1 = A(r, t) \sin\theta + B(r, t) \cos\theta, \tag{3.9}$$

where the amplitudes A and B satisfy the equations

$$\frac{\partial \nabla_1^2 A}{\partial t} + \frac{1}{r}(B \nabla_1^2 \psi_0' - \psi_0' \nabla_1^2 B) = 0 \tag{3.10a}$$

$$\frac{\partial \nabla_1^2 B}{\partial t} - \frac{1}{r}(A \nabla_1^2 \psi_0' - \psi_0' \nabla_1^2 A) = -\psi_0', \tag{3.10b}$$

and

$$\nabla_1^2 = \frac{\mathrm{d}^2}{\mathrm{d}r^2} + \frac{1}{r}\frac{\mathrm{d}}{\mathrm{d}r} - \frac{1}{r^2}.$$

It is convenient to reduce (3.10a, b) to one equation for the complex amplitude $C = A + \mathrm{i}B$:

$$\frac{\partial \nabla_1^2 C}{\partial t} + \frac{\mathrm{i}}{r}(\psi_0' \nabla_1^2 C - C \nabla_1^2 \psi_0') = -\mathrm{i}\psi_0'. \tag{3.11}$$

Integrating (3.11) with respect to r from 0 to r and using the identities

$$\psi_0' \nabla_1^2 C - C \nabla_1^2 \psi_0' = \frac{1}{r}[r(\psi_0' C' - C\psi_0'')]', \tag{3.12a}$$

$$\nabla_1^2 C = \frac{1}{r^2}[r(rC' - C)]' \tag{3.12b}$$

we obtain
$$\frac{\partial}{\partial t}(rC'-C)+\mathrm{i}(C'\psi_0'-C\psi_0'')=-\frac{\mathrm{i}}{r}\int_0^r r^2\psi_0'\,\mathrm{d}r. \tag{3.13}$$

When integrating we took into account that
$$C=C'(0)r \quad \text{for} \quad r\to 0, \tag{3.14}$$
which follows from the regularity of ∇C and $\nabla\psi_0$ at $r=0$. (An analysis like the above can also be used to demonstrate the f-plane stability of vortices to low mode perturbations and is presented in Appendix B.)

Dividing by r^2 then yields
$$\frac{\partial C_1'}{\partial t}+\mathrm{i}(C_1'\bar{\psi}_2-C_1\bar{\psi}_2')=-\mathrm{i}F, \tag{3.15}$$

where
$$C_1=\frac{C}{r};\quad \bar{\psi}_2=\frac{\psi_0'}{r};\quad F=\frac{1}{r^3}\int_0^r r^2\psi_0'\,\mathrm{d}r, \tag{3.16}$$
the primes again denoting differentiation with respect to r.

Equation (3.15) is now Laplace transformed, and (3.6c) is used, to yield a time transform variable
$$\tilde{C}_1(P)=\int_0^\infty \mathrm{e}^{-Pt}C_1(r,t)\,\mathrm{d}t. \tag{3.17}$$

The resulting equation is easily solved to obtain
$$\tilde{C}_1=-\mathrm{i}(P+\mathrm{i}\bar{\psi}_2)\int_0^r\frac{F\,\mathrm{d}r}{P(P+\mathrm{i}\bar{\psi}_2)^2}+R(P)(P+\mathrm{i}\bar{\psi}_2), \tag{3.18}$$
where $R(P)$ is an arbitrary function of the transform parameter P. This function can be found from the condition of boundedness of C_1 (and, consequently, $\tilde{C}_1$) for $r\to\infty$. Assuming that ψ_0' decays sufficiently rapidly as $r\to\infty$, e.g.
$$\psi_0'\leqslant O(1/r^2),\quad r\to\infty, \tag{3.19}$$
the integral in (3.18) converges for large r and we have
$$R(P)=\mathrm{i}\int_0^\infty\frac{F\,\mathrm{d}r}{P(P+\mathrm{i}\bar{\psi}_2)^2}. \tag{3.20}$$

Thus
$$\tilde{C}_1=\mathrm{i}(P+\mathrm{i}\bar{\psi}_2)\int_r^\infty\frac{F\,\mathrm{d}r}{P(P+\mathrm{i}\bar{\psi}_2)^2}. \tag{3.21}$$

The solution C can be readily obtained by applying the inverse Laplace transformation to (3.21) and has the form
$$C=A+\mathrm{i}B=r\left[\mathrm{i}t\int_r^\infty F\mathrm{e}^{-\mathrm{i}\bar{\psi}_2 t}\,\mathrm{d}r-\bar{\psi}_2\int_0^t t\left(\int_r^\infty F\mathrm{e}^{-\mathrm{i}\bar{\psi}_2 t}\,\mathrm{d}r\right)\mathrm{d}t\right]. \tag{3.22}$$

It is useful also to calculate the quantity
$$\nabla_1^2C=\nabla_1^2A+\mathrm{i}\nabla_1^2B=r(\mathrm{e}^{-\mathrm{i}\bar{\psi}_2 t}-1)-\nabla_1^2\psi_0'\int_0^t t\left(\int_r^\infty F\mathrm{e}^{-\mathrm{i}\bar{\psi}_2 t}\,\mathrm{d}r\right)\mathrm{d}t. \tag{3.23}$$

Thus, by virtue of (3.5), (3.7a) and (3.9) the $O(\alpha)$ streamfunction and vorticity fields are equal to
$$\psi_1=(A+\bar{Y}_0\psi_0')\sin\theta+(B+\bar{X}_0\psi_0')\cos\theta, \tag{3.24a}$$
$$\nabla^2\psi_1=(\nabla_1^2A+\bar{Y}_0\nabla_1^2\psi_0')\sin\theta+(\nabla_1^2B+\bar{X}_0\nabla_1^2\psi_0')\cos\theta, \tag{3.24b}$$
respectively, where A and B are given by (3.22). According to (3.24a,b), the $O(\alpha)$ field is a sum of two dipoles with mutually perpendicular axes and amplitudes depending on

time and distance from the vortex centre. This sum is thus also a dipole, but with a time-dependent axis, amplitude and structure. The vortex moves owing to its interaction with this dipole. We now calculate the trajectory of the vortex due to these interactions.

4. Definition of vortex trajectories and velocities

The velocity and, consequently, the trajectory of the vortex is not unique, but rather is subject to the choice of a characteristic point of the vortex, which we subsequently track. It is natural to consider the motion of the points corresponding to the extrema of relative and potential vorticity and of the streamfunction.

4.1. *The relative vorticity extremum*

The relative vorticity of the vortex to $O(\alpha^2)$ is

$$\zeta = \zeta_0(r) + \alpha \nabla^2 \psi_1(r, t), \tag{4.1}$$

where $\zeta_0 = \nabla^2 \psi_0(r)$. In the coordinate system whose origin coincides with the relative vorticity extremum, we have

$$\nabla \zeta|_{r=0} = \zeta_0' \nabla r|_{r=0} + \alpha \nabla(\nabla^2 \psi_1)|_{r=0} = 0. \tag{4.2}$$

Let the initial field $\psi_0(r)$ be regular at $r = 0$ up to the third derivative. Thus, $\zeta'_{0|r=0} = 0$ and it can be readily found from (4.2), (3.24*b*), and (3.23) that

$$\bar{Y}_0^{\zeta} + \mathrm{i}\bar{X}_0^{\zeta} = \int_0^t t\left(\int_0^{\infty} F \mathrm{e}^{-\mathrm{i}\bar{\psi}_2 t}\,\mathrm{d}r\right)\mathrm{d}t - \frac{1}{\zeta_0''}(\mathrm{e}^{-\mathrm{i}\psi_{00}'' t} - 1) \tag{4.3a}$$

$$V_0^{\zeta} + \mathrm{i}U_0^{\zeta} = \dot{\bar{Y}}_0^{\zeta} + \mathrm{i}\dot{\bar{X}}_0^{\zeta} = t\int_0^{\infty} F \mathrm{e}^{-\mathrm{i}\bar{\psi}_2 t}\,\mathrm{d}r + \mathrm{i}\frac{\psi_{00}''}{\zeta_{00}''}\mathrm{e}^{-\mathrm{i}\psi_{00}'' t}, \tag{4.3b}$$

where

$$\psi_{00}'' \equiv \psi_0''(0), \quad \zeta_{00}'' = \zeta_0''(0) \tag{4.3c}$$

and the overdot implies a time derivative.

Formulae (4.3) determine the trajectory and velocity of the relative vorticity extremum; it can be verified that they coincide with those calculated by the method proposed by Sutyrin (1988).

4.2. *The streamfunction extremum*

To obtain the velocity and trajectory of the streamfunction extremum, it is necessary only to substitute ψ for ζ in (4.1) and (4.2). The resulting trajectory and velocity are given by the formulae

$$\bar{Y}_0^{\psi} + \mathrm{i}\bar{X}_0^{\psi} = \int_0^t t\left(\int_0^{\infty} F \mathrm{e}^{-\mathrm{i}\bar{\psi}_2 t}\,\mathrm{d}r\right)\mathrm{d}t - \frac{\mathrm{i}t}{\psi_{00}''}\int_0^{\infty} F \mathrm{e}^{-\mathrm{i}\bar{\psi}_2 t}\,\mathrm{d}r, \tag{4.4a}$$

$$V_0^{\psi} + \mathrm{i}U_0^{\psi} = \dot{\bar{Y}}_0^{\psi} + \mathrm{i}\dot{\bar{X}}_0^{\psi} = t\int_0^{\infty} F \mathrm{e}^{-\mathrm{i}\bar{\psi}_2 t}\,\mathrm{d}r - \frac{i}{\psi_{00}''}\int_0^{\infty} F \mathrm{e}^{-\mathrm{i}\bar{\psi}_2 t}\,\mathrm{d}r - \frac{t}{\psi_{00}''}\int_0^{\infty} \bar{\psi}_2\, \bar{Y}_2\, F \mathrm{e}^{-\mathrm{i}\bar{\psi}_2 t}\,\mathrm{d}r. \tag{4.4b}$$

4.3. *Fluid particle trajectory and velocity*

One can also define the trajectory and velocity of the vortex by tracing the path of a particular fluid particle in the vortex core. For example, typhoons are often modelled using the azimuthal velocity profile.

$$V_2 = A r \mathrm{e}^{-r} \tag{4.5}$$

(cf. Chan & Williams 1987; Fiorino & Elsberry 1989). Obviously the corresponding relative vorticity

$$\zeta = A(2-r)\,\mathrm{e}^{-r} \tag{4.6}$$

has a weak singularity at $r = 0$, because $\nabla\zeta$ is not continuous at this point. Note that the relative vorticity is maximal at $r = 0$ but (4.3*a*, *b*) of §4.1 are inapplicable since $\zeta_0'|_{r=0} \neq 0$. (Note, however, that (4.4*a*, *b*) for the streamfunction extremum remain valid.)

Potential vorticity conservation shows that the above singularity always moves with its initial parcel fluid. This implies that

$$\left.\frac{\partial\psi}{\partial y}\right|_{r=0} = -U, \quad \left.\frac{\partial\psi}{\partial x}\right|_{r=0} = V \tag{4.7}$$

in the coordinate system attached to the potential vorticity extremum. From (3.24*a*), (4.7) we have

$$\left.\frac{B+\bar{X}_0\psi_0'}{r}\right|_{r=0} = \dot{\bar{Y}}_0; \quad \left.\frac{A+\bar{Y}_0\psi_0'}{r}\right|_{r=0} = -\dot{\bar{X}}_0, \tag{4.8}$$

whence it follows that

$$\frac{\mathrm{d}}{\mathrm{d}t}(\bar{Y}_0+\mathrm{i}\bar{X}_0)+\mathrm{i}\psi_{00}''(\bar{Y}_0+\mathrm{i}\bar{X}_0) = -\left.\frac{\mathrm{i}C}{r}\right|_{r=0}. \tag{4.9}$$

By virtue of (3.22)

$$-\left.\frac{\mathrm{i}C}{r}\right|_{r=0} = \hat{f}+\mathrm{i}\psi_{00}''\hat{f}, \tag{4.10}$$

where

$$\hat{f} = \int_0^t t\left(\int_0^\infty F\mathrm{e}^{-\mathrm{i}\bar{\psi}_2 t}\,\mathrm{d}r\right)\mathrm{d}t. \tag{4.11}$$

Substituting (4.10) into (4.9) we obtain

$$\bar{Y}_0+\mathrm{i}\bar{X}_0 = \int_0^t t\left(\int_0^\infty F\mathrm{e}^{-\mathrm{i}\bar{\psi}_2 t}\,\mathrm{d}r\right)\mathrm{d}t, \quad V_0+\mathrm{i}U_0 = t\int_0^\infty F\mathrm{e}^{-\mathrm{i}\bar{\psi}_2 t}\,\mathrm{d}r. \tag{4.12a, b}$$

Equation (4.7) shows that (4.12a, b) are applicable also for a non-singular vorticity field, in which case they describe the motion of the fluid particle initially located at $r = 0$.

5. Asymptotic regimes

5.1. *Asymptotics for $r \to \infty$, t fixed*

Let us assume that the azimuthal velocity ψ_0' decays sufficiently rapidly so that the net angular momentum M,

$$M = \int_0^\infty r^2\psi_0'\,\mathrm{d}r, \tag{5.1}$$

is finite. This requires that

$$\psi_0' \leqslant o(1/r^3), \quad r\to\infty. \tag{5.2}$$

and thus the function F in (3.16) is equal to

$$F = M/r^3 + o(1/r^3), \quad r\to\infty. \tag{5.3}$$

It follows that

$$\int_r^\infty F\mathrm{e}^{-\mathrm{i}\bar{\psi}_2 t}\,\mathrm{d}r = \frac{M}{2r^2}+o(1/r^2), \quad r\to\infty. \tag{5.4}$$

Using (5.4) we readily obtain the asymptotic expression for C:

$$C = A + \mathrm{i}B = \mathrm{i}\frac{M}{2r}t + o(1/r). \tag{5.5}$$

One can see from (5.5), (3.24a) and (5.2) that the behaviour of streamfunction ψ_1 at large r is determined by the net angular momentum M. If $M \neq 0$ then

$$A = o(1/r), \quad B = tM/2r, \quad r \to \infty, \tag{5.6a}$$

i.e. the cosine dipole in (3.24a) decays much more rapidly than the sine dipole for large r. For $M = 0$ we have

$$A = o(rF_1), \quad B = trF_1 + o(rF_1), \quad r \to \infty, \tag{5.6b}$$

where

$$F_1 = \int_r^\infty F\,\mathrm{d}r = -\frac{1}{r^2}\int_0^r r\psi_0\,\mathrm{d}r. \tag{5.7}$$

It is seen that in this case the correction field ψ_1 decays approximately as the streamfunction ψ_0 for $r \to \infty$, i.e. much more rapidly than for non-zero angular momentum M. This is in agreement with the numerical results of Shapiro & Oyama (1990) which showed that the vortex with zero M stays much more localized than in the case of $M \neq 0$. Note also that both dipole components in (3.24a) decay identically.

It is important to note that by virtue of (3.23), the relative vorticity $\nabla^2\psi_1$ is *always localized*, as its decay is governed by ψ_0' and $\nabla_1^2\psi_0'$, rather than M.

5.2. *Trajectory and velocity of the vortex for $t \to \infty$*

We now consider the behaviour of the vortex trajectory and velocity at times much larger than the characteristic turnover time T_* (see §2). It is seen from (4.3), (4.4) and (4.12) that vortex trajectory is determined by the integral

$$R = \int_0^\infty F\mathrm{e}^{-\mathrm{i}\bar{\psi}_2 t}\,\mathrm{d}r, \tag{5.8}$$

and, therefore, to calculate the trajectories and velocities for large times we have to estimate this integral for $t \to \infty$. Details of these calculations are given in Appendix A and here we give only the final results. It is important to note that the trajectories and velocities (4.3), (4.4) and (4.12) of the various characteristic points of the vortex accurately track each other for large t.

The case of non-zero M

Not surprisingly, the vortex motion at large times depends strongly on the value of M. If $M \neq 0$ then the value of the integral (5.8) is strongly affected by the periphery of the initial vortex state $\psi_0(r)$, which agrees with the conclusions, based on numerical experiments, of Fiorino & Elsberry (1989). Below we consider some typical and frequently applied decay laws for ψ_0 at larger r.

(i) *Algebraic decay*

$$\psi_0 \approx a/r^K, \quad r \to \infty, \tag{5.9}$$

where $K > 2$ and a is a constant. Here, vortex trajectories and velocity are given by

$$V_0 + \mathrm{i}U_0 \approx S_K t^{K/(K+2)}, \quad \bar{Y}_0 + \mathrm{i}\bar{X}_0 \approx S_K \frac{K+2}{2(K+1)} t^{2(K+1)/(K+2)}, \tag{5.10a, b}$$

where
$$S_K = \frac{M\Gamma(2/(K+2))}{(K\alpha)^{2/(K+2)}(K+2)} e^{i\pi/(K+2)} \tag{5.10c}$$

and Γ represents the standard gamma function. Equation (5.10*a*) shows that the vortex is always accelerated, with the acceleration increasing for increasing K (i.e. for more confined vortices). Since $K > 2$ the magnitude of the zonal velocity ($|\bar{U}_0|$) is always smaller than the magnitude of the meridional velocity ($|\bar{V}_0|$). The vortex trajectory is a straight line, $\bar{Y}_0 = m\bar{X}_0$, with slope

$$m = \cot(\pi/(K+2)). \tag{5.11}$$

Note that the slope m becomes large for large K, meaning that more confined vortices move on a more purely meridional path.

(ii) *Exponential-algebraic decay*

$$\psi_0 = ar^u e^{-r}, \quad r \to \infty, \tag{5.12}$$

where a and u are constants. In this case

$$V_0 + iU_0 = \frac{M}{2}\left(\frac{t}{\ln^2 t} + i\frac{\pi t}{\ln^3 t}\right), \quad \bar{Y}_0 + i\bar{X}_0 = \frac{M}{4}\left(\frac{t^2}{\ln^2 t} + i\frac{\pi t^2}{\ln^3 t}\right). \tag{5.13a, b}$$

The vortex moves, and accelerates, along the trajectory

$$\bar{Y}_0 = \frac{1}{\pi}\bar{X}_0 \ln(|\bar{X}_0|^{\frac{1}{2}}). \tag{5.13c}$$

Such a curve approaches purely meridional motion for large time.

(iii) *Gaussian–algebraic decay*

$$\psi_0 = ar^u e^{-r^2}, \quad r \to \infty. \tag{5.14}$$

Vortex motion here is analogous to the preceding case, but is slightly faster:

$$\bar{V}_0 + i\bar{U}_0 \approx \frac{M}{2}\left(\frac{t}{\ln t} + i\frac{\pi t}{2\ln^2 t}\right), \quad \bar{Y}_0 + i\bar{X}_0 = \frac{M}{4}\left(\frac{t^2}{\ln t} + i\frac{\pi t}{2\ln^2 t}\right). \tag{5.15a, b}$$

The vortex trajectory has the form

$$\bar{Y}_0 = \frac{1}{\pi}\bar{X}_0 \ln|\bar{X}_0|, \tag{5.15c}$$

which is steeper meridionally than (5.13*c*).

It is important to note that in all the above cases, the general direction of vortex motion is determined by the sign of the net angular momentum M; cyclones ($M > 0$) move to the north-northwest and anticyclones ($M < 0$) to the south-southwest.

The case of vanishing net angular momentum; $M = 0$

It readily follows from (5.1) that if $M = 0$, number of points, $r_0^{(K)}$, $K = 1, 2, \ldots$, exist such that

$$\bar{\psi}_2'(r_0^{(K)}) = 0. \tag{5.16}$$

The number of points satisfying (5.16) depends on the profile and can be either finite or infinite. It can be shown by stationary phase analysis (see Appendix A) that the value of the integral (5.8) is largely determined by the contributions around the points

in (5.16). Suppose for simplicity that the profile $\bar{\psi}_2(r)$ has only one point r_0 satisfying (5.16). Then

$$\bar{V}_0+\mathrm{i}\bar{U}_0 \approx St^{\frac{1}{2}}\mathrm{e}^{-\mathrm{i}[\bar{\psi}_2(r_0)t+\alpha]}, \quad \bar{Y}_0+\mathrm{i}\bar{X}_0 \approx \frac{\mathrm{i}S}{\bar{\psi}_2(r_0)}t^{\frac{1}{2}}\mathrm{e}^{-\mathrm{i}[\bar{\psi}_2(r_0)t+\alpha]}, \tag{5.17a, b}$$

where

$$S=\left(\frac{2\pi}{|\bar{\psi}_2''(r_0)|}\right)^{\frac{1}{2}}F(r_0); \quad \alpha=[\operatorname{sign}\bar{\psi}_0''(r_0)]\tfrac{1}{4}\pi. \tag{5.17c}$$

It readily follows from (5.17*b*) that the vortex with $M=0$ tends to move along a widening spiral curve for large t (cf. Willoughby 1992).

Finally, note in the above formulae that the form of the vortex trajectories at large times independent is of M, although the vortex propagation velocities are proportional to it.

5.3. *Asymptotics of the streamfunction and vorticity for $t\to\infty$, r fixed*

By virtue of (3.24*a*) the behaviour of the $O(\alpha)$ streamfunction ψ_1 is determined by the function

$$\hat{C}(r,t)=C+\psi_0'(\bar{Y}_0+\mathrm{i}\bar{X}_0). \tag{5.18}$$

Recall that

$$\bar{Y}_0+\mathrm{i}\bar{X}_0=\int_0^t t\left(\int_0^\infty F\,\mathrm{e}^{-\mathrm{i}\bar{\psi}_2 t}\,\mathrm{d}r\right)\mathrm{d}t+S(t), \tag{5.19}$$

where the function $S(t)$ depends on the definition of velocity (cf. (4.3*a*), (4.4*a*) and (4.12*a*)). After some algebra, (5.18) and (5.19) yield

$$\hat{C}=\mathrm{i}r\left(V_0+\mathrm{i}U_0-\frac{\mathrm{d}S}{\mathrm{d}t}\right)-\mathrm{i}tr\int_0^r F\,\mathrm{e}^{-\mathrm{i}\bar{\psi}_2 t}\,\mathrm{d}r+\psi_0'\int_0^t t\left(\int_0^r F\mathrm{e}^{-\mathrm{i}\bar{\psi}_2 t}\,\mathrm{d}r\right)\mathrm{d}t+S\psi_0'. \tag{5.20}$$

Consider now the form of the perturbation streamfunction in a system attached to the moving vortex, i.e.

$$\begin{aligned}\psi_1^m &= \psi_1+U_0 r\sin\theta-V_0 r\cos\theta\\ &= (A+\bar{Y}_0\psi_0'+U_0 r)\sin\theta+(B+\bar{X}_0\psi_0'-V_0 r)\cos\theta.\end{aligned} \tag{5.21}$$

The behaviour of ψ_1^m thus is determined by the function

$$C_1(r,t)=\hat{C}-\mathrm{i}r(V_0+\mathrm{i}U_0), \tag{5.22}$$

which is equal to

$$C_1(r,t)=-\mathrm{i}tr\int_0^r F\mathrm{e}^{-\mathrm{i}\bar{\psi}_2 t}\,\mathrm{d}r+\psi_0'\int_0^t t\left(\int_0^r F\mathrm{e}^{-\mathrm{i}\bar{\psi}_2 t}\,\mathrm{d}r\right)\mathrm{d}t-\mathrm{i}r\frac{\mathrm{d}S}{\mathrm{d}t}+\psi_0'S. \tag{5.23}$$

The relative vorticity $\nabla^2\psi_1$ of the correction field is determined by the quantity $\nabla_1^2\hat{C}$, which equals

$$\nabla_1^2\hat{C}=r(\mathrm{e}^{-\mathrm{i}\bar{\psi}_2 t}-1)+\nabla_1^2\psi_0'\int_0^t t\left(\int_0^r F\mathrm{e}^{-\mathrm{i}\bar{\psi}_2 t}\,\mathrm{d}r\right)\mathrm{d}t+S\nabla_1^2\psi_0' \tag{5.24}$$

by virtue of (3.23) and (5.19). Note that $\nabla^2\psi_1\equiv\nabla^2\psi_1^m$ and with these definitions we can write the equation defining ψ_1 (i.e. (3.4*a*)) as

$$\frac{\partial}{\partial t}\nabla^2\psi_1^m+J(\nabla^2\psi_1^m,\psi_0)+J(\psi_1^m,\nabla^2\psi_0)+\psi_{0x}=0. \tag{5.25}$$

We now consider the behaviour of the functions C_1 and $\nabla_1^2\hat{C}$ at a fixed r for $t\to\infty$.

First, suppose $\bar{\psi}_2$, $\bar{\psi}_2'$ do not vanish, which of course is possible only if the net angular momentum M differs from zero. After some algebra we have

$$C_1 = -\psi_0' \int_0^r \frac{F}{\bar{\psi}_2^2}\mathrm{d}r - \mathrm{i}r\frac{\mathrm{d}S}{\mathrm{d}t} + S\psi_0' + O(t^{-1}), \tag{5.26}$$

$$C_1' = -\psi_0'' \int_0^r \frac{F}{\bar{\psi}_2^2}\mathrm{d}r - \frac{rF}{\bar{\psi}_2} - \mathrm{i}\left(r\frac{\mathrm{d}S}{\mathrm{d}t}\right)' + (S\psi_0')' + O(t^{-1}), \tag{5.27}$$

$$\nabla_1^2 \hat{C} = r(\mathrm{e}^{-\mathrm{i}\bar{\psi}_2 t} - 1) - \nabla_1^2\psi_0'\left[\frac{F}{\bar{\psi}_2\bar{\psi}_2'}\mathrm{e}^{-\mathrm{i}\bar{\psi}_2 t} + \int_0^r \frac{F}{\bar{\psi}_2^2}\mathrm{d}r\right] + S\nabla_1^2\psi_0' + O(t^{-1}), \tag{5.28}$$

$$(\nabla_1^2 \hat{C})' = \mathrm{i}t\frac{F\nabla_1^2\psi_0' - r\bar{\psi}_2\bar{\psi}_2'}{\bar{\psi}_2}\mathrm{e}^{-\mathrm{i}\bar{\psi}_2 t} + O(1) \tag{5.29}$$

for $t \to \infty$. It readily follows from (5.26), (5.27) and (5.28) that the streamfunction ψ_1^m and the velocity field in the moving coordinate system are bounded for $t \to \infty$ although the vortex increases as $t \to \infty$ (see §5.2).

Thus, the $J(\psi_1^m, \nabla^2\psi_0)$ term in (5.25) remains bounded for large t, which implies that the third, fourth and fifth terms in (3.4*a*) approximately compensate each other.

The relative vorticity, $\nabla^2\psi_1$, is also bounded for $t \to \infty$ (see (5.28)); however, its spatial derivatives grow proportionally to t by virtue of (5.29). This implies that the inhomogeneous terms in (3.4*b*), which create the next-order correction ψ_2, grow with time. Thus, in the case $M \neq 0$, our theory is valid for

$$\alpha t \ll 1, \tag{5.30}$$

i.e. for times much smaller than the 'wave' timescale $1/\beta L$.

In the case of $M = 0$ the asymptotics for $t \to \infty$ become somewhat more complicated. For $r > r_0$, where r_0 is the first zero of $\bar{\psi}_2$, the functions C_1, C_1' and $\nabla_1^2\hat{C}$ behave as $t^{\frac{1}{2}}$. However, in the central part of the vortex, for $r < r_0$, the functions C_1, C_1' and $\nabla_1^2\hat{C}$ are also bounded and, therefore, the streamfunction and velocities in the moving system remain finite there also. Thus, it follows from our theory that for sufficiently large times the vortex (i.e. for $r < r_0$) is simply advected by the flow induced by the β-gyres. In the far field (i.e. $r > r_0$) the flow strengthens and broadens with increasing time. This result is well confirmed by numerical experiments (cf. Fiorino & Elsberry 1989, and the next section).

6. Numerical verification

As a test of the analysis, we have performed a sequence of numerical initial value problems employing

$$\frac{\partial}{\partial t}\nabla^2\psi + J(\psi, \nabla^2\psi + \beta y) = \nabla\cdot\nu\nabla\nabla^2\psi \tag{6.1}$$

subject to the initial condition (2.2) and the boundary conditions of no normal flow and free-slip (i.e. $\psi = 0$ and $\nabla^2\psi = 0$ on the boundaries). Equation (6.1) is effectively (2.1) (save for the presence of viscosity ν). The solutions of (2.1) were obtained using finite difference techniques and a closed domain. The Jacobian was computed using a fourth-order-accurate energy- and enstrophy-conserving Arakawa formulation. The viscous parameter ν was assigned a constant value over the greater part of the domain. For the 10 grid points nearest the boundaries, its magnitude was ramped up by a factor of 9. This combination of closed boundaries and viscosity had the effect of reducing the impact of wave radiation and reflection.

Our solution method consisted of solving the vorticity equation for the streamfunction

$$\nabla^2\psi = q, \tag{6.2}$$

where, at a given time level, q was known. The inversion was obtained by sine transforming (6.2) in one spatial dimension, solving the resulting tridiagonal matrix equation, for each wavenumber, directly and inverse transforming the result back to the physical space domain. The sine transform was chosen in view of the boundary conditions mentioned above. The result of this procedure was used to move the model state forward. Time stepping was performed by the leapfrog technique with averaging of adjacent time levels every 100th time step to suppress computational mode instability. Viscous effects were lagged one time step.

Most of our experiments were conducted with a grid spacing of 10 km, a time step of 900 s and a value of the viscosity (in the centre of the domain) of 10^6 cm^2 s^{-1}. The total domain size was 2560×2560 km. A series of experiments has been conducted in which the values of above parameters were varied, and have demonstrated that none of the results to be reported here depend upon our particular choices.

The discrete extrema in potential vorticity, vorticity and streamfunction were located in the numerical grid at each time step. In order to locate the absolute extrema when it was between grid points, a two-dimensional parabolic profile was fit by a least-squares method to the 3×3 matrix of values surrounding the extrema. Thus we obtained numerical predictions for the extrema value and extrema trajectories, which were subsequently stored for comparison with the theory.

The theoretical predictions for the extrema trajectories were obtained by numerically evaluating (4.3), (4.4) and (4.12). These in turn required computing integrals of the vortex streamfunction over the infinite domain. This was performed by breaking the integral into a near-field and a far-field part, where the break was made typically at a radius of 10 eddy lengthscales. The far-field integral was then transformed to a finite domain by use of the variable $1/r$. All integrals were computed according to Romberg's technique to at least an accuracy of 1 part in 10000.

It was found from both the numerical solutions of (6.1) and from the evaluations of the theoretical formulae that the differences in the various extrema trajectories were insignificant. Therefore, we will show here only comparisons between the numerical and analytical results for the streamfunction extrema.

6.1. *Gaussian vortices*

Figure 1 compares the trajectories of a Gaussian vortex, whose profile is given by (5.14) with $u = 0$. The dimensional characterization of this vortex was chosen crudely from oceanic considerations, i.e. it corresponds to a vortex of maximum swirl speed of 200 cm s^{-1} at a radius of 600 km. As such, these parameters represent a stronger eddy than is typically observed. We have performed experiments for weaker eddies; the results shown here are the most restrictive with respect to the length of time for which the theory is adequate. The turnover timescale for this eddy is approximately 8 hours ($\frac{1}{3}$ day), while the associated wave timescale is $(\beta L)^{-1} \approx 9.6$ days. The corresponding value of parameter $\alpha = \beta L^2/V$ is 0.035, so the vortex is well suited for the theory. The marks on the trajectories correspond to time intervals of one day, from which it is seen that the quantitative comparison is quite acceptable up to the wave timescale. The error in predicted position after 9 days is roughly 30% in meridional (-94 km *vs.* -74 km) and 20% in zonal (-55 km *vs.* -45 km) displacement, with the theoretical prediction being consistently too large. These results are surprisingly good as the theory is meant to hold only for times short compared to the wave timescale.

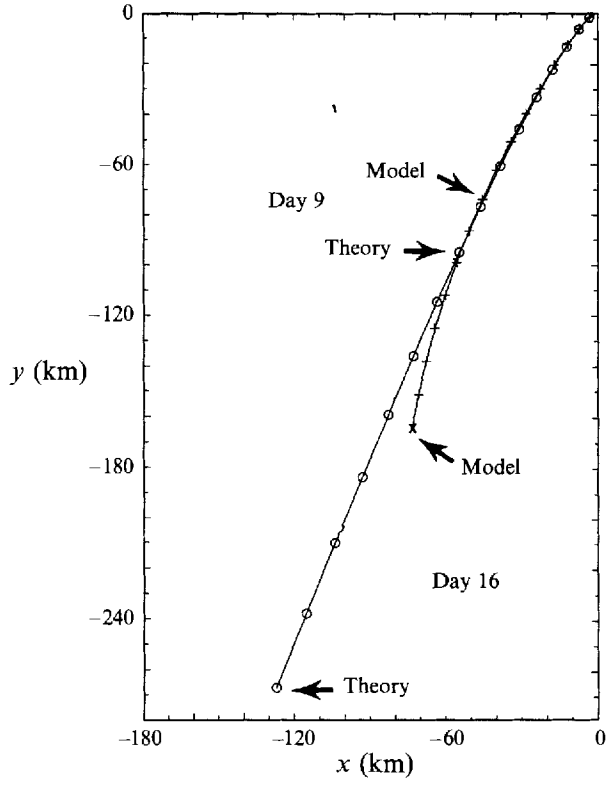

FIGURE 1. Gaussian vortex trajectory test. Time intervals of a day are indicated. The theoretical trajectory is marked by circles and the numerical trajectory by crosses. Sixteen days are shown.

It is also interesting that the structure of the trajectory is well represented by the theory, even if the amplitude of the displacement is off. This appears in figure 1, where it is evident that the direction of the theoretical displacement accurately predicts the model displacement.

A major reason for the discrepancy also emerges from the computations. The theory assumes $\psi_0 = \psi_0(r)$, thereby neglecting any loss in amplitude of the mean-state vortex. On the other hand, a significant wave field develops and the potential vorticity field in the vicinity of the eddy is warped considerably; both perturbations draw their energy from the vortex. The numerical solutions of (6.1) include these processes and thus the vortex amplitude decreases over the course of the experiment. For example, the maximum streamfunction amplitude from the numerical experiment in figure 1 has dropped by 20% by day 9.

The mean-state vortex feeds directly into the trajectory speeds (cf. (4.4)). The retention of a 'too-strong' vortex leads naturally to the theory predicting displacements which are too large. The shapes of the trajectories are less sensitive to vortex amplitude (cf. (5.15)), which provides a partial explanation for why the trajectory structure is well represented.

6.2. *Hurricane profiles*

We have also compared trajectories based on the classical hurricane profile, whose swirl velocity v is given by $v = Ar\mathrm{e}^{-r}$ (see figure 2). The physical parameters of this vortex were consistent with a swirl speed of 20 m s^{-1} at a radius of 100 km. The vortex timescale is thus about 84 minutes, and the wave timescale is about 5.7 days. The

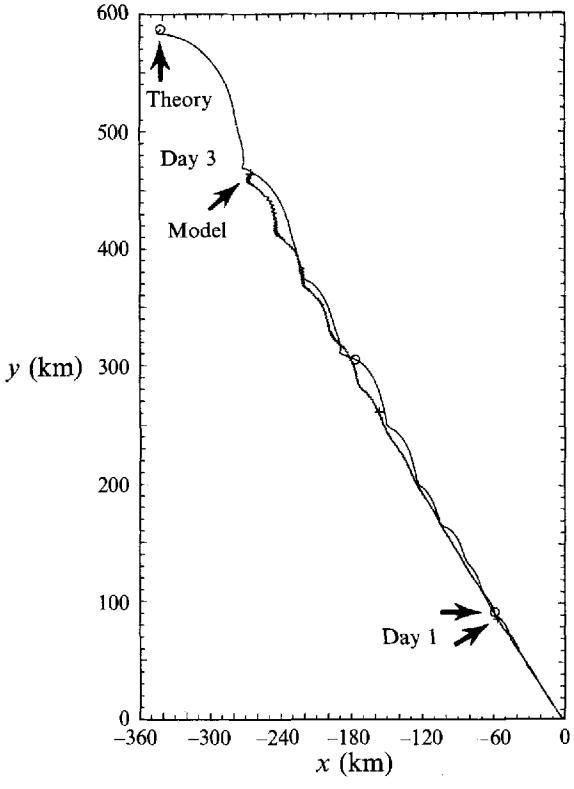

FIGURE 2. Same as figure 1, except that a hurricane profile is used.

comparison in figure 2 shows an acceptable agreement out to about 3 days (displacement errors of 28% meridionally and 26% zonally). During this time, the vortex has moved a net distance of ~ 520 km ($\sim$ 5–6 lengthscales), which differs considerably from the previous case, where the vortex moved ~ 1.5 eddy scales before the errors became larger than $\sim 30\%$. Thus the present theory yields useful information in a wide variety of circumstances.

Again, the theoretical predictions are too large and, again, this difference can be at least partly ascribed to the unrealistically strong theoretical eddy. By $2\frac{1}{2}$ days, the numerical hurricane streamfunction has decreased in amplitude by 12%, a change unaccounted for by the theory.

It is also interesting that the trajectory shape is well represented by the theory. This applies even to the reproduction of the gentle 'cusps' which appear. Note that in both tracks such cusps are initially absent, and then grow in magnitude with increasing time.

6.3. $M = 0$

Both previous profiles possessed considerable net angular momentum, $M = \iint r\psi \, \mathrm{d}r$. We now present the results of a comparison of the theory with a profile characterized by $M = 0$. Specifically, we used

$$\psi = a(2 - r^2/r_0^2)\, \mathrm{e}^{-r^2/r_0^2}, \tag{6.3}$$

where the formula is presented dimensionally. This vortex is the weakest discussed so far, corresponding to a swirl speed of 100 cm s^{-1} at 60 km. Many of the formulae

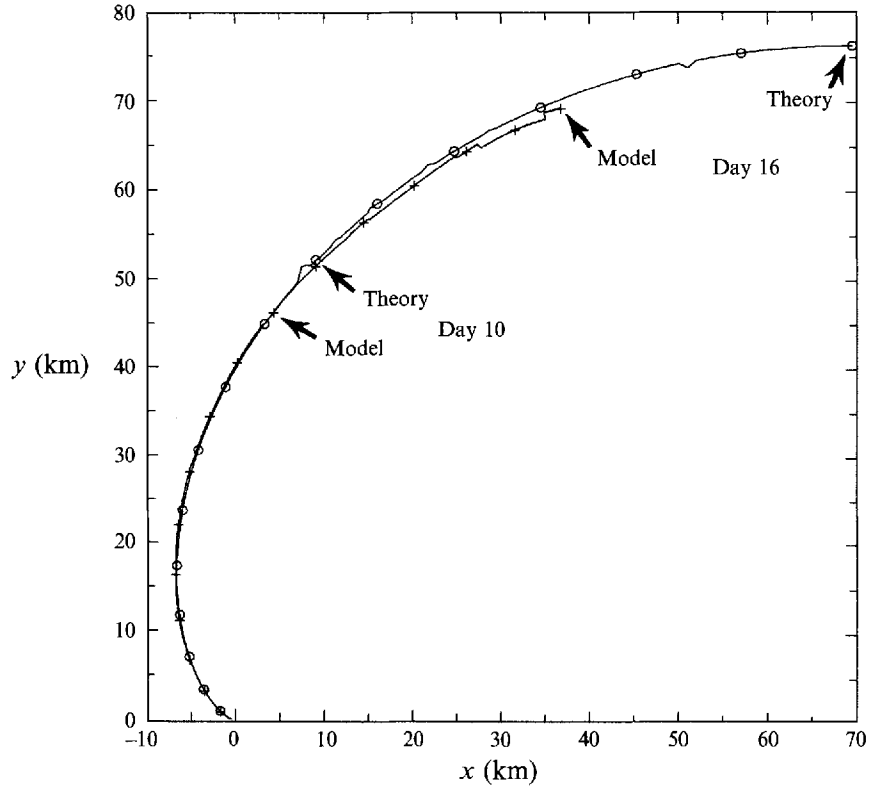

FIGURE 3. Same as figure 1, except a profile with $M = 0$ is used.

depend strongly on M for their behaviour (cf. (5.13)), thus this comparison provides a strong test of the utility of this theory.

The trajectory comparisons are given in figure 3 and confirm this experiment as the most successful of any of the tests. This is particularly interesting as the eddy timescale is roughly 1.2 days, so $\alpha \approx 0.13$. This is the largest value of α shown here, so the theory should be the least applicable. Figure 3 displays the results of 16 days of numerical integration, after which time the meridional displacement error is $\sim 10\%$ (-76 km *vs.* -69 km), while the zonal displacement error is much worse (90%). This latter measure is slightly misleading as the net zonal displacement is small (~ 36 km). Perhaps it is more telling that the trajectory shape is remarkably well modelled. This bears on the question of zonal error, as the zonal displacement actually curves back on itself and passes through zero after about 9 days.

Thus the predictions of the present theory with respect to vortex trajectory are born out by numerical experimentation. The notable results to emerge here are that the theory holds up to times comparable to a wave timescale, in spite of the formal restriction to much smaller times, and the trajectory shapes are quite well captured for even longer times. The best comparisons are found for $M = 0$. This is in keeping with the theory, whose far-field predictions improve considerably in this case. A source of theoretical error appears to be its lack of amplitude loss, which results in the theoretical predictions being too large.

7. Far-field radiation

Since ψ_0, $\nabla^2\psi_0$, and $\nabla^2\psi_1$ decay rapidly for $r\to\infty$ (see §5.1), one might approximate (3.4*b*) in this region by

$$\frac{\partial\nabla^2\psi_2}{\partial t}=-\frac{\partial\psi_1}{\partial x}. \tag{7.1}$$

However, if the net angular momentum M is different from zero, then it follows from (5.5) and (3.4*d*) that

$$\psi_2=-\tfrac{1}{16}Mt^2\cos 2\theta \quad \text{for} \quad r\to\infty. \tag{7.2}$$

Hence, ψ_2 has an infinite energy and enstrophy, which is physically unacceptable.

The difficulty here is that for non-zero M, the expansion (3.2) is not valid throughout the plane. Specifically, the non-divergent planetary waves outside the vortex can move with arbitrarily large group velocities; hence far-field radiation cannot be neglected, even for times much smaller than the 'wave' timescale $(\beta L)^{-1}$ (see also Reznik 1992). Equivalently, in the proper expression of the far-field dynamics, terms like $\partial\nabla^2\psi_1/\partial t$ and $\alpha\,\partial\psi_1/\partial x$ are really of the same order. Consideration of these points suggests that the expansion for the far-field streamfunction has the form

$$\psi=\alpha^2\hat{\psi}_1(X,Y,t)+\alpha^3\hat{\psi}_2(X,Y,t)+\ldots, \tag{7.3}$$

where $(X,Y)=\alpha(x,y)$. Such a dependence on the 'slow' variables X, Y is due to the fact that only sufficiently long planetary waves, with wavelengths $\gtrsim 1/\alpha$ can approach the far-field on times $t\ll 1/\alpha$.

Thus, the plane is divided into two regions: Region I ($r\sim 1$) in which the representation (3.2) is valid, and Region II ($r\sim 1/\alpha$) in which the streamfunction is represented in the form (7.3). The expansions (3.2) and (7.3) must be joined in an intermediate region by using the method of asymptotic matching (e.g. Van Dyke 1964).

The solution for $\hat{\psi}_1$ in (7.3) is obtained in a manner similar to that in Reznik (1992). Specifically, substituting (7.3) into (2.5) and (2.2) we obtain the equation

$$\frac{\partial\overline{\nabla^2}\hat{\psi}_1}{\partial t}+\frac{\partial\hat{\psi}_1}{\partial x}=0, \tag{7.4a}$$

where

$$\overline{\nabla^2}=\frac{\partial^2}{\partial X^2}+\frac{\partial^2}{\partial Y^2},$$

and the initial condition

$$\hat{\psi}_1|_{t=0}=0. \tag{7.4b}$$

When deriving (7.4*a*) we assume that the initial streamfunction $\psi_0(r)$ decays sufficiently rapidly for large r that $\psi_0(r)\ll\alpha$ as $r=O(\alpha^{-1})$. We also require for large r that $\hat{\psi}_1$ be bounded, i.e.

$$\hat{\psi}_1<\infty \quad \text{as} \quad R\to\infty \tag{7.4c}$$

where $R=(X^2+Y^2)^{\frac{1}{2}}$. To match the expansions (3.2) and (7.3) for small R, we rewrite $\alpha\psi_1(r,t)$ and $\alpha^2\hat{\psi}_1(X,Y,t)$ in terms of the intermediate variables $\xi=\alpha^\gamma x$, $\eta=\alpha^\gamma y$, $0<\gamma<1$ and let α tend to zero for fixed ξ and η (cf. Van Dyke 1964). Taking (5.5) into account, we have

$$\alpha\psi_1\approx\alpha^{1+\gamma}\frac{Mt}{2\tilde{R}}\cos\theta, \tag{7.5}$$

where $\tilde{R} = \alpha^{\gamma} r$. In order that the analogous limit for $\alpha^2 \hat{\psi}_1(X, Y, t)$ coincides with (7.5), it is necessary that

$$\hat{\psi}_1 \to \frac{Mt}{2R} \cos\theta \quad \text{as} \quad R \to 0. \tag{7.6}$$

The relationship (7.6) constitutes a second boundary condition on $\hat{\psi}_1$.

The solution to (7.4) was obtained by Reznik (1992) and has the form

$$\hat{\psi}_1 = M\pi \frac{\partial G}{\partial X}, \tag{7.7a}$$

where

$$G(X, Y, t) = -\frac{1}{\pi}\left(\frac{t}{R}\right)^{\frac{1}{2}} \int_0^{\infty} \frac{J_1\{2[Rt(u^2 + \cos^2\frac{1}{2}\theta)]^{\frac{1}{2}}\}\, \mathrm{d}u}{[(u^2+1)(u^2+\cos^2\frac{1}{2}\theta)]^{\frac{1}{2}}}. \tag{7.7b}$$

The far-field streamfunction does not have a dipole structure, as occurs for ψ_1 in (3.9); rather, the far-field solution describes an oscillatory sequence reflecting the dispersive wave behaviour of (7.4*a*). The function $\hat{\psi}_1$ in (7.7*a*) tends to $O(r^{-\frac{3}{2}})$ as $r \to \infty$ and, therefore, the composite uniformly valid expansion for the lowest-order correction field ψ_c, of form (cf. Van Dyke 1964)

$$\psi_c = \alpha\psi_1(r, \theta, t) + \alpha^2 \hat{\psi}_1(R, \theta, t) - \alpha \frac{Mt}{2r} \cos\theta, \tag{7.8}$$

has finite energy and enstrophy. Another important property of the far-field solution is that it ensures the boundedness of the net angular momentum of the evolving vortex. To see this, note that the contribution

$$M_c = \int_0^{2\pi} \mathrm{d}\theta \int_0^{\infty} r^2 \frac{\partial \psi_c}{\partial r} \mathrm{d}r \tag{7.9}$$

to the net angular momentum due to the correction field (7.8) is finite. (If (7.9) is evaluated without taking into account the far-field radiation, the integral diverges because of (5.6)).

8. Conclusions

We have analytically investigated the evolution of an intense, circular barotropic vortex on the β-plane. The proposed asymptotic theory is formally valid for times of the order of a few turnover times. In practice, the theory is often accurate for several turnover times, as confirmed by the numerical experiments described in §6. For strong oceanic and atmospheric eddies the prediction time is of the order of 10 days and 2–3 days, respectively. Both are comparable to the wave timescale. If $M = 0$, we have found the theory to work well for times greater than the wave timescale.

This theory differs from the preceding theories by Sutyrin & Flierl (1994), Smith & Ulrich (1990) and Smith & Weber (1993). One of the main difficulties of the theory of barotropic vortices has been calculating the solution to (3.4*a*, *c*), which govern the β-gyre behaviour. Sutyrin & Flierl (1994) solved this problem for a vortex with piecewise-constant potential vorticity. Smith and colleagues simplified the problem by assuming that the sum of the third, fourth and fifth terms in (3.4*a*) was smaller than the rest of the terms and could be included in the next-order approximation. Smith & Ulrich (1990), for example, supposed that the third, fourth and fifth terms in (3.4*a*)

approximately cancel each other, consistent with the numerical experiments which suggest that the vortex is simply advected by the β-gyres. Smith & Weber (1993) assumed that the spatial gradient of the initial relative vorticity is of the order of β.

In contrast, we present here the solution of the complete equation (3.4a), subject to both (3.4c) and an arbitrary initial vortex. One property of this solution is that the sum

$$J(\psi_1, \nabla^2\psi_0) - U_0\frac{\partial\nabla^2\psi_0}{\partial x} - V_0\frac{\partial\nabla^2\psi_0}{\partial y}$$

is generally not smaller than the other terms in (3.4a).

We are also able to determine exactly the trajectories of particular points of the vortex (e.g. points associated with relative vorticity or streamfunction extrema, or a given fluid particle in the vortex core). These various trajectories differ insignificantly from each other. The vortex velocity and trajectory, however, depend critically on the net angular momentum M. Anticyclones ($M < 0$) move southwestward and cyclones ($M > 0$) northwestward. The special case of a vortex with $M = 0$ moves on a more complex trajectory depending on the structure of the central part of the vortex. The initial westward motion of the vortex eventually reverses to the east (see also Willoughby 1992).

A third, important distinction is that we have calculated the motion in the far-field created by the radiated planetary waves. This region does not significantly influence the vortex trajectory for the times considered here ($T \ll (\beta L)^{-1}$) but it plays an important role in the solution by ensuring the regularity of higher-order approximations and boundedness of the net angular momentum. The intensity of the radiated field is proportional to M; for $M = 0$ the radiation can be neglected.

A shortcoming of the present analysis is that at this level of approximation, the changes in the vortex structure and intensity are not taken into account. It is therefore generally the case that the vortex amplitude used in the theory is larger than that realized by the numerical computations; hence, the theory predicts vortex velocities which are faster than the numerical vortex. This is a problem which gets worse as time progresses, and the numerical vortices reduce in amplitude. To include such effects might require analysis of higher-order approximations. This, of course, is not simple and is the subject of further investigation.

This work was initiated during a visit by G. M. R. to Rutgers State University and finished during a visit to the Florida State University. G. M. R. gratefully acknowledges the hospitality of the host institutions during these trips. W. K. D. is supported by NSF grant OCE-9012114, NASA grant NAGW-3087 and ONR contract N00014-89-J-1577. Sheila Heseltine prepared the manuscript and the computer graphics were prepared by J. Park.

Appendix A

Let us represent the integral (5.8) in the form

$$R = R_1 + R_2,$$

here

$$R_1 = \int_0^A F e^{-i\bar{\psi}_2 t}\,dr; \quad R_2 = \int_A^\infty F e^{-i\bar{\psi}_2 t}\,dr \tag{A 1}$$

and A is large enough so that the function $\bar{\psi}_2$ is monotonic and (5.3) is valid on the interval $[A, \infty]$.

We now estimate R_2 as $t\to\infty$. Let M be non-zero; then by virtue of (5.3) we have

$$R_2 \approx M\bar{R}_2; \quad \bar{R}_2 = \int_A^\infty \frac{1}{r^3} e^{-i\bar{\psi}_2 t}\, dr. \tag{A 2}$$

Let $\bar{\psi}_2$ increase monotonically from some negative value to zero. Introducing the new variable $z = -\bar{\psi}_2$ we obtain

$$\bar{R}_2 = \int_0^{z_A} \frac{e^{izt}}{r^3(z)\,\bar{\psi}_2'(r(z))}\, dz. \tag{A 3}$$

Consider now various large-r behaviours for ψ_0.

(i) Algebraic decay

$$\psi_0 = a/r^K, \quad K>2, \quad r\to\infty. \tag{A 4}$$

In this case $\bar{\psi}_2 = -Ka/r^{K+2}$ and we have

$$\bar{R}_2 = \frac{1}{(K+2)(Ka)^{2/(K+2)}} \int_0^{z_A} \frac{e^{izt}}{z^{K/(K+2)}}\, dz. \tag{A 5}$$

Introducing the new variable $\vartheta = zt$ into integral (A 5) and using the formula (Gradshteyn & Ryzhik 1965)

$$\int_0^\infty \frac{e^{i\vartheta}}{\vartheta^\alpha}\, d\vartheta = \Gamma(1-\alpha)\, e^{i\pi(1-\alpha)/2}, \tag{A 6}$$

where $\Gamma(x)$ is gamma-function, we obtain

$$R_2 \approx \frac{M\Gamma(2/(K+2))}{(K+2)(Ka)^{2/(K+2)}} e^{i\pi/(K+2)}\, t^{-2/(K+2)}, \quad t\to\infty. \tag{A 7}$$

To analyse the case of exponentially decreasing ψ_0, we use the asymptotic result

$$\int_0^B \frac{\cos\vartheta t}{\vartheta\,|\ln^m\vartheta|}\, d\vartheta = \frac{1}{(m-1)\ln^{m-1} t} + O(\ln^{-m} t), \tag{A 8}$$

$$\int_0^B \frac{\sin\vartheta t}{\vartheta\,|\ln^m\vartheta|}\, d\vartheta = \tfrac{1}{2}\pi \frac{1}{\ln^m t} + O(\ln^{-m-1} t) \tag{A 9}$$

as $t\to\infty$.

(ii) Exponential decay

$$\psi_0 \approx a\, e^{-r}/r^\alpha, \quad r\to\infty. \tag{A 10}$$

For large r we have $r^3\bar{\psi}_2' \approx -z\ln^3 z$ and, therefore,

$$R_2 \approx \frac{M}{2}\int_0^{z_A} \frac{e^{-izt}}{z\,|\ln^3 z|}\, dz \approx \tfrac{1}{2}M\left(\frac{1}{\ln^2 t} + i\frac{\pi}{\ln^3 t}\right) \tag{A 11}$$

as $t\to\infty$.

(iii) Gaussian decay

$$\psi_0 \approx [a\, e^{-r^2}]/r^\alpha, \quad r\to\infty. \tag{A 12}$$

In this case, $r^3\bar{\psi}_2' \approx 2z\ln^2 z$ for large r, and

$$R_2 \approx \frac{M}{2}\int_0^{z_A} \frac{e^{izt}}{z\ln^2 z}\, dz \approx \frac{M}{2}\left(\frac{1}{\ln t} + \frac{i\pi}{2\ln^2 t}\right) \quad \text{as} \quad t\to\infty. \tag{A 13}$$

Now let $M = 0$. Then the function F (see (3.16)) can be represented as

$$F = -\frac{1}{r^3}\int_r^\infty r^2\bar{\psi}_0' \,\mathrm{d}r. \tag{A 14}$$

Using (A 14) one can readily show that in the case of algebraic decay for $\bar{\psi}_0$ (see (A 4))

$$R_2 = \frac{(aK)^{2/(K+2)}}{K^2-4}\Gamma\left(\frac{K}{K+2}\right)[\mathrm{e}^{-\mathrm{i}\pi K/2(K+2)}]\, t^{-K/(K+2)} \tag{A 15}$$

as $t \to \infty$. For the more rapid decay laws (A 10) and (A 12)

$$R_2 = O(1/t), \quad t \to \infty. \tag{A 16}$$

Note that in these cases, the function R_2 decreases more rapidly than $t^{-\frac{1}{2}}$, i.e.

$$R_2 = O(t^{-\frac{1}{2}}), \quad t \to \infty. \tag{A 17}$$

We now estimate the integral R_1 for $t \to \infty$. The function F is regular for $r \in [0, A]$ and, therefore,

$$R_1 = O(t^{-1}), \quad t \to \infty \tag{A 18}$$

if $\bar{\psi}_2' \neq 0$ throughout the interval $[0, A]$. Let $\bar{\psi}_2'$ be zero at some point $r_0 \in [0, A]$, and, for simplicity, suppose this is the only such point. Then the main contribution to R_1 comes from the neighbourhood of the point r_0. Evaluating this contribution by stationary phase yields

$$R_1 \approx \frac{1}{t^{\frac{1}{2}}}\left(\frac{2\pi}{|\bar{\psi}_2''(r_0)|}\right)^{\frac{1}{2}} F(r_0)\,\mathrm{e}^{-\mathrm{i}[\bar{\psi}_2(r_0)\,t + \operatorname{sign}\bar{\psi}_0''(r_0)\,\pi/4]} \tag{A 19}$$

for $t \to \infty$.

It readily follows from (A 7), (A 11), (A 13), (A 18) and (A 19) that when $M \neq 0$ the integral R_2 prevails in R for large t, and for $M = 0$ the integral R_1 determines the behaviour of R.

Appendix B. Analytical proof of the f-plane stability of an arbitrary two-dimensional circular vortex relative to perturbations of azimuthal mode number 1

Let us write the equation for the streamfunction

$$\frac{\partial \nabla^2\psi}{\partial t} + J(\psi, \nabla^2\psi) = 0, \tag{B 1}$$

and represent ψ in the form

$$\psi = \bar{\psi}_0(r) + \tilde{\psi}(r, \theta, t), \tag{B 2}$$

where $\bar{\psi}_0(r)$ is the basic state and $\tilde{\psi}(r, \theta, t)$ a perturbation to this state. Assuming that

$$\tilde{\psi} = C(r)\,\mathrm{e}^{\mathrm{i}(\theta - \sigma t)} \tag{B 3}$$

and linearizing (B 1) we obtain

$$-\sigma\nabla_1^2 C + \frac{1}{r}(\bar{\psi}_0'\nabla_1^2 C - C\nabla^2\bar{\psi}_0') = 0. \tag{B 4}$$

The amplitude C must satisfy the boundary conditions

$$C = 0 \quad \text{at} \quad r = 0, \tag{B 5}$$

$$C = o(1/r), \quad r \to \infty. \tag{B 6}$$

Using the identities (3.12*a*, *b*) and conditions (B 5) and (B 6), we can integrate (B 4) over r and obtain the equation

$$C'(\bar{\psi}' - \sigma r) - C(\bar{\psi}_0'' - \sigma) = 0, \tag{B 7}$$

whence it follows that

$$C = A(\bar{\psi}_0' - \sigma r). \tag{B 8}$$

Obviously, the function C can satisfy (B 5) and (B 6) only when $\sigma = 0$, i.e. the perturbation (B 3) cannot grow (see also Gent & McWilliams 1986).

REFERENCES

ADEM, J. 1956 A series solution for the barotropic vorticity equation and its application to the study of atmospheric vortices. *Tellus* **8**, 364.

BOGOMOLOV, V. A. 1977 The dynamics of vorticity on a sphere. *Izv. Akad. Nauk SSSR, Mekh. Zhid. Gaza* **13**, 57.

BOGOMOLOV, V. A. 1979 On the two-dimensional hydrodynamics on a sphere. *Izv. Akad. Nauk SSSR, Mekh. Phys. Atmos. Okeana* **15**, 29.

BOGOMOLOV, V. A. 1985 On the vortex motion on a rotating sphere. *Izv. Akad. Nauk SSSR, Mekh. Phys. Atmos. Okeana* **21**, 391.

CHAN, J. C. L. & WILLIAMS, R. T. 1987 Analytical and numerical studies of the beta-effect in tropical cyclone motion. Part I: Zero mean flow. *J. Atmos. Sci.* **44**, 1257.

FIORINO, M. & ELSBERRY, R. L. 1989 Some aspects of vortex structure related to tropical cyclone motion. *J. Atmos. Sci.* **46**, 975.

FIRING, E. & BEARDSLEY, R. 1976 The behaviour of a barotropic eddy on a β-plane. *J. Phys. Oceanogr.* **6**, 57.

GENT, P. R. & MCWILLIAMS, J. C. 1996 The instability of barotropic circular vortices. *Geophys. Astrophys. Fluid Dyn.* **35**, 209.

GRADSHTEYN, S. & RYZHIK, I. W. 1965 *Tables of Integrals, Series and Products*, 4th Edn. Academic.

MCWILLIAMS, J. C. & FLIERL, G. R. 1979 On the evolution of isolated, nonlinear vortices. *J. Phys. Oceanogr.* **9**, 1155.

PEDLOSKY, J. 1986 *Geophysical Fluid Dynamics*. Springer.

PENG, M. & WILLIAMS, R. T. 1990 Dynamics of vortex asymmetries and their influence on vortex motion on a β-plane. *J. Atmos. Sci.* **47**, 1987.

REZNIK, G. M. 1990 On motion of point vortex on a beta-plane. *Oceanology* **30**, 707 (in Russian).

REZNIK, G. M. 1992 Dynamics of singular vortices on a beta-plane. *J. Fluid Mech.* **240**, 405.

REZNIK, G. M. & KRAVTSOV, S. A. 1994 Analytical study of singular barotropic vortex on a beta-plane. *J. Fluid Mech.* (submitted).

ROSS, R. J. & KURIHARA, Y. 1992 A simplified scheme to simulate asymmetries due to the beta effect in barotropic vortices. *J. Atmos. Sci.* **49**, 1620.

SHAPIRO, L. J. & OOYAMA, K. V. 1990 Barotropic vortex evolution on a beta-plane. *J. Atmos. Sci.* **47**, 170.

SMITH, R. K. & ULRICH, W. 1990 An analytical theory of tropical cyclone motion using a barotropic model. *J. Atmos. Sci.* **47**, 1973.

SMITH, R. K. & WEBER, M. C. 1993 An extended analytical theory of tropical-cyclone motion in a barotropic shear flow. *Q. J. Met. Soc.* (submitted).

SUTYRIN, G. G. 1988 Motion of an intense vortex on a rotating globe. *Fluid Dyn.* **23**, 215.

SUTYRIN, G. G. 1989 Forecast of intense vortex motion with an azimuthal modes model. In *Mesoscale/Synoptic Coherent Structures in Geophysical Turbulence* (ed. J. C. J. Nihoul & B. M. Jamart), p. 771. Elsevier.

SUTYRIN, G. G. & FLIERL, G. R. 1994 Intense vortex motion on the beta-plane. Part I. Development of the beta-gyres. *J. Atmos. Sci.* (submitted).

VAN DYKE, M. 1964 *Perturbation Methods in Fluid Mechanics*. Academic.

WILLOUGHBY, M. E. 1992 Linear motion of a shallow-water barotropic vortex as an initial-value problem. *J. Atmos. Sci.* **49**, 2015.